Thermoelastic Coupling Vibration Characteristics of the Axially Moving Beam With Frictional Contact

Guo Xu-Xia[1]
School of Sciences,
Xi'an University of Technology,
710048 Xi'an, P.R.C.;
Department of Mechanical and Electrical Engineering,
Baoji University of Arts and Sciences,
721007 Baoji, P.R.C.
e-mail: gxx5432106@sina.com

Wang Zhong-Min
School of Sciences,
Xi'an University of Technology,
710048 Xi'an, P.R.C.

The thermoelastic coupling vibration characteristics of the axially moving beam with frictional contact are investigated. The piecewise differential equation of motion for the axially moving beam in the thermoelastic coupling case and the continuous conditions at the contact point are established. The eigenequation is derived by the differential quadrature method, and the first order dimensionless complex frequencies of the simply supported axially moving beam under the coupled thermoelastic case are calculated. The effects of the dimensionless thermoelastic coupling factor, the dimensionless moving speed, the spring stiffness, the friction coefficient, and the normal pressure on the thermoelastic coupling vibration characteristics of the axially moving beam with frictional contact are discussed. [DOI: 10.1115/1.4001513]

Keywords: thermoelastic coupling, axially moving beam, frictional contact, vibration characteristics, differential quadrature method

1 Introduction

The vibration characteristics of moving systems have played an important part in many engineering systems, such as aerial lifter, transmission belt, magnetic tape, band saw, and weave fiber. Many contributions on axially moving media can be found in the literature. Simpson [1] studied the natural frequencies of the axially moving beam with a clamped boundary by the eigenvalue method. Wickert and Mote [2] investigated the vibration characteristic of the moving string and beam under the simply supported and clamped boundary conditions. In the second paper [3], they develop a complex modal analysis for continuous systems using a first order partial differential equation with respect to time. Chakraborty and Mallik [4] analyzed the linear and nonlinear free vibrations of the simply supported axially moving beam by wave propagation. Kong and Parker [5] researched the free vibration of the axially moving beam with small flexural stiffness. The asymptotic solutions of natural frequencies are obtained by the perturbation method of the algebraic equation. Yang [6] studied the natural frequencies of axially moving beams by the method of multiple scales. The results show that the natural frequencies are affected by the axial motion and proportional to the square of the velocity of the axially moving beam.

The above mentioned researches are all in the stable temperature field; the impacts of the thermoelastic coupling are ignored. But in the most actual engineering systems, the impacts of the thermoelastic coupling effect need to be taken into consideration. The bending of the beam is inevitably affected by the temperature changes in the elastic vibration; the vibration characteristics and dynamics of the beam will be changed due to the variation in temperature [7,8]. For this reason, the thermal conduction equation involving the deformation term and the motion equation must be solved simultaneously. Chang and Wan [9] studied the nonlinear coupled thermoelastic vibration of the isotropic rectangular thin plate under all kinds of boundary conditions by the Berger assumption. Eslami et al. [10] analyzed the coupled thermoelastic problems based on the first order shell theory of the Love assumption. Copper and Pilkey [11] presented a thermoelastic solution technique for beams with arbitrary quasi-static temperature distributions that create large transverse normal and shear stresses. Guo and Rogerson [12] studied the thermoelastic coupling in a doubly clamped elastic prism beam and examined its size dependence. Sun et al. [13] studied the thermoelastic damping in microbeam resonators. The results show that the amplitude of deflection and the thermal moment are attenuated and that the vibration frequency is increased with the thermoelastic coupling effect being considered. Guo et al. [14] analyzed the coupled thermoelastic vibration for the axially moving beam by the differential quadrature method (DQM). The curves of the real parts and the imaginary parts of the first three order dimensionless complex frequencies versus the dimensionless axially moving speed are obtained.

For the axially moving beam considered in this paper, the frictional contact makes the problem more complicated. In all the papers cited above, the effects of the friction in the systems were not considered. However, the friction force is a kind of nonconservative force of many engineering systems and produces an important influence upon the vibration characteristics of the systems [15]. Cheng and Perkins [16] studied the stability of a traveling string subject to large dry friction and reported that dry friction induces flutter instability in the high speed range. Chen [17] studied the natural frequencies and stability of an axially traveling string in contact with a stationary load system. The results show that the inertia in the stationary load system tends to decrease the natural frequencies of all modes of the system in the subcritical speed range; the effects of stiffness are opposite to those of the inertia. Adams [18] analyzed the self-excited oscillations of the beam in sliding with a constant friction coefficient. Mottershead and Chan [19] studied the flutter instability of circular disks with frictional follower loads. Daniel et al. [20] analyzed the vibrations induced by friction in moving continua and their application to brake squeal, showing that the brake disk should not be too large in order to avoid very low critical speeds. Gottfried et al. [21] used a discretization approach for the modeling and stability analysis of an axially moving beam for a clamped beam with frictional contact.

[1]Corresponding author.

Contributed by the Technical Committee on Vibration and Sound of ASME for publication in the JOURNAL OF VIBRATION AND ACOUSTICS. Manuscript received September 20, 2009; final manuscript received March 22, 2010; published online August 26, 2010. Assoc. Editor: Jean Zu.

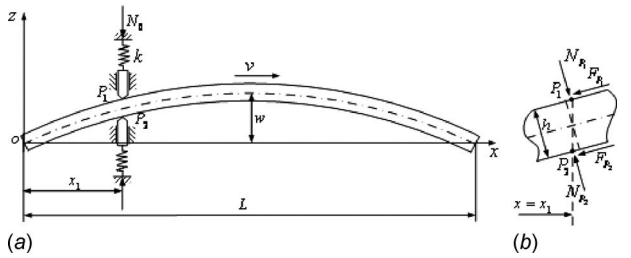

Fig. 1 Axially moving beam with frictional contact in the temperature field. (*a*) The model of the beam with frictional contact. (*b*) Traverse and normal forces of the contact points.

In this paper, the thermoelastic coupling vibration of the axially moving Bernoulli–Euler beam with frictional contact is analyzed, the piecewise differential equation of motion of the beam is established based on the generalized thermoelastic and vibration theory, and the continuous conditions at the contact point are provide. The eigenequation is obtained by the differential quadrature method, and the dimensionless complex frequencies of the axially moving beam with frictional contact are calculated. The thermoelastic coupling vibration characteristics of the axially moving beam with frictional contact are obtained.

2 The Piecewise Differential Equation of Motion and the Continuous Conditions

Consider an elastic rectangular beam moving with constant speed v in the x direction, as shown in Fig. 1. The beam has the length L, width b, and thickness h in the x, y, and z directions, respectively, the density of the material is ρ, and the Young's modulus is E. We denote the initial temperature of the beam as $\tau_0=\tau(x,z,t_0)$, and the temperature of the instantaneous time t is $\tau_1=\tau_1(x,z,t)$, so the temperature changes of the beam is $T=\tau_1-\tau_0$. We shall neglect frictional heating. The beam slides through an elastically supported guide at an axial position $x=x_1$. The top and bottom parts of the guide are assumed to be identical. The top and bottom surfaces of the guide are assumed to remain in contact with the beam due to the relatively large normal force N_0 applied externally. k is the spring stiffness, μ is the friction coefficient, and $w=w(x,t)$ is the displacement in the z direction.

Due to the normal pressure and the tangential friction force at the contact points P_1 and P_2, we have to consider two different segments of the beam, namely, $[x_0,x_1]$ and $[x_1,x_2]$, where $x_0=0$ and $x_2=L$. We assumed that $w_n(x,t)$ $(n=1,2)$ are the deflections of every segment, so the differential equation of motion and the continuous conditions at $x=x_1$ are then [14]

$$EI\frac{\partial^4 w_n}{\partial x^4}+\frac{\partial^2 M_T}{\partial x^2}+\rho A\left(\frac{\partial^2 w_n}{\partial t^2}+2v\frac{\partial^2 w_n}{\partial x\,\partial t}+v^2\frac{\partial^2 w_n}{\partial x^2}\right)=0,\quad x_{n-1}\le x\le x_n,\quad n=1,2 \tag{1}$$

$$\begin{gathered} w_1(x_1^-,t)=w_2(x_1^+,t)\\ \frac{\partial w_1(x_1^-,t)}{\partial x}=\frac{\partial w_2(x_1^+,t)}{\partial x}\\ EI\left[\frac{\partial^2 w_1(x_1^-,t)}{\partial x^2}-\frac{\partial^2 w_2(x_1^+,t)}{\partial x^2}\right]+\bar{M}=0\\ EI\left[\frac{\partial^3 w_1(x_1^-,t)}{\partial x^3}-\frac{\partial^3 w_2(x_1^+,t)}{\partial x^3}\right]+\bar{N}=0 \end{gathered} \tag{2}$$

where $M_T=bE\alpha_T\int_{-h/2}^{h/2}Tz\,dz$ is the thermal moment, $A=bh$ is the area of the cross-section, $\bar{M}$ is the resultant couple and $\bar{N}$ is the transverse resultant force at $x=x_1$.

According to the small deformation of the beam, we use $\theta=\partial w/\partial x$, $\cos\theta\approx 1$, and $\sin\theta\approx\theta$ throughout the paper. We assume the applicability of Coulomb's law of friction, and from Fig. 1(*b*) we know that the moment produced by the normal forces is small; it is ignored in order to simplify the calculations, so the transverse force, the friction force, and the couple by the friction force at $x=x_1$ are given by

$$N_{P_1}=N_0+kw_1(x_1^-,t)+F_{P_1}w_1'(x_1^-,t)$$

$$F_{P_1}=\mu N_{P_1} \tag{3}$$

$$N_{P_2}=N_0-kw_1(x_1^-,t)-F_{P_2}w_1'(x_1^-,t)$$

$$F_{P_2}=\mu N_{P_2} \tag{4}$$

$$M_{P_1}=\tfrac{1}{2}\mu hN_{P_1}$$

$$M_{P_2}=\tfrac{1}{2}\mu hN_{P_2} \tag{5}$$

From Eq. (3), we obtain

$$\begin{aligned} N_{P_1}&=\frac{1}{[1-\mu w_1'(x_1^-,t)]}[N_0+kw_1(x_1^-,t)]\approx[1+\mu w_1'(x_1^-,t)][N_0\\ &\quad+kw_1(x_1^-,t)]=N_0+kw_1(x_1^-,t)+\mu N_0w_1'(x_1^-,t)\\ &\quad+\mu kw_1(x_1^-,t)w_1'(x_1^-,t) \end{aligned} \tag{6}$$

The term $\mu kw_1(x_1^-,t)w_1'(x_1^-,t)$ in Eq. (6) is small, and it is disregarded; N_{P_1} can be expressed as

$$N_{P_1}=N_0+kw_1(x_1^-,t)+\mu N_0w_1'(x_1^-,t) \tag{7}$$

In the same way, N_{P_2} can be given by

$$N_{P_2}=N_0-kw_1(x_1^-,t)-\mu N_0w_1'(x_1^-,t) \tag{8}$$

Equation (5) can be rewritten as

$$\begin{aligned} M_{P_1}&=\tfrac{1}{2}\mu h[N_0+kw_1(x_1^-,t)+\mu N_0w_1'(x_1^-,t)]\\ M_{P_2}&=\tfrac{1}{2}\mu h[N_0-kw_1(x_1^-,t)-\mu N_0w_1'(x_1^-,t)] \end{aligned} \tag{9}$$

Then, $\bar{N}$ and $\bar{M}$ can be written as

$$\begin{aligned} \bar{N}&=N_{P_1}-N_{P_2}=2kw_1(x_1^-,t)+2\mu N_0w_1'(x_1^-,t)\\ \bar{M}&=M_{P_2}-M_{P_1}=\mu h[-kw_1(x_1^-,t)-\mu N_0w_1'(x_1^-,t)] \end{aligned} \tag{10}$$

Introducing Eq. (10) into Eq. (2), the continuous conditions become

$$\begin{gathered} w_1(x_1^-,t)=w_2(x_1^+,t)\\ \frac{\partial w_1(x_1^-,t)}{\partial x}=\frac{\partial w_2(x_1^+,t)}{\partial x}\\ EI\left[\frac{\partial^2 w_1(x_1^-,t)}{\partial x^2}-\frac{\partial^2 w_2(x_1^+,t)}{\partial x^2}\right]+\mu h[-kw_1(x_1^-,t)-\mu N_0w_1'(x_1^-,t)]=0\\ EI\left[\frac{\partial^3 w_1(x_1^-,t)}{\partial x^3}-\frac{\partial^3 w_2(x_1^+,t)}{\partial x^3}\right]+2kw_1(x_1^-,t)+2\mu N_0w_1'(x_1^-,t)=0 \end{gathered} \tag{11}$$

The thermal conduction equation containing the thermoelastic coupling term of the beam is

$$\frac{\partial T}{\partial t} - a\frac{\partial^2 T}{\partial z^2} + \frac{E\alpha_T \tau_0}{\rho c_v}\frac{\partial}{\partial t}\left(-z\frac{\partial^2 w_n}{\partial x^2}\right) = 0, \quad x_{n-1} \le x \le x_n, \quad n = 1,2 \tag{12}$$

where $a = \gamma/\rho c_v$ is the thermal diffusivity, γ is the thermal conductivity, and c_v is the specific heat at a constant volume.

For the convenience, the dimensionless quantities are introduced as follows:

$$\xi = \frac{x}{L}, \quad \varsigma = \frac{x_1}{L}, \quad \bar{z} = \frac{z}{h}, \quad \bar{w} = \frac{w}{h}, \quad \bar{T} = \frac{T}{\tau_0}, \quad \bar{t} = \sqrt{\frac{E}{\rho}}\frac{t}{L}, \quad c = \sqrt{\frac{\rho}{E}}v, \quad K = \frac{kL^3}{EI}, \quad F = \frac{N_0 L^2}{EI} \tag{13}$$

Substituting Eq. (13) into Eqs. (1), (11), and (12), we can get the dimensionless forms

$$\frac{h^2}{12L^2}\frac{\partial^4 \bar{w}_n}{\partial \xi^4} + \alpha_T \tau_0 \frac{\partial^2 \bar{M}_T}{\partial \xi^2} + \left(\frac{\partial^2 \bar{w}_n}{\partial \bar{t}^2} + 2c\frac{\partial^2 \bar{w}_n}{\partial \xi\, \partial \bar{t}} + c^2\frac{\partial^2 \bar{w}_n}{\partial \xi^2}\right) = 0$$

$$\frac{\partial^2 \bar{T}}{\partial \bar{z}^2} - \frac{h^2}{aL}\sqrt{\frac{E}{\rho}}\frac{\partial \bar{T}}{\partial \bar{t}} + \frac{E\alpha_T h^4}{a\rho c_v L^3}\sqrt{\frac{E}{\rho}}\frac{\partial^3 \bar{w}_n}{\partial \xi^2\, \partial \bar{t}} = 0$$

$$(x_{n-1} \le x \le x_n, \quad n = 1,2) \tag{14}$$

where $\bar{M}_T = \int_{-1/2}^{1/2} \bar{T}\bar{z}\,d\bar{z}$

$$\bar{w}_1(\varsigma^-, \bar{t}) = \bar{w}_2(\varsigma^+, \bar{t})$$

$$\frac{\partial \bar{w}_1(\varsigma^-, \bar{t})}{\partial \xi} = \frac{\partial \bar{w}_2(\varsigma^+, \bar{t})}{\partial \xi} \tag{15}$$

$$\left[\frac{\partial^2 \bar{w}_1(\varsigma^-, \bar{t})}{\partial \xi^2} - \frac{\partial^2 \bar{w}_2(\varsigma^+, \bar{t})}{\partial \xi^2}\right] - \mu^2 F \bar{w}_1'(\varsigma^-, \bar{t}) - \mu K \bar{w}_1(\varsigma^-, \bar{t}) = 0$$

$$\left[\frac{\partial^3 \bar{w}_1(\varsigma^-, \bar{t})}{\partial \xi^3} - \frac{\partial^3 \bar{w}_2(\varsigma^+, \bar{t})}{\partial \xi^3}\right] + 2K\bar{w}_1(\varsigma^-, \bar{t}) + 2\mu F \bar{w}_1'(\varsigma^-, \bar{t}) = 0$$

In order to analyze the vibration characteristics of the beam, we may assume that all quantities change harmonically in Eq. (14), i.e.,

$$\overline{w_n}(\xi, \bar{t}) = W_n(\xi)e^{j\omega \bar{t}}$$

$$\bar{T}(\bar{z}, \bar{t}) = T^*(\bar{z})e^{j\omega \bar{t}} \qquad (\xi_{n-1} \le \xi \le \xi_n, \quad n = 1,2) \tag{16}$$

where $j = \sqrt{-1}$ and ω is the dimensionless complex frequency of the axially moving beam under the thermoelastic coupling case. Substituting Eq. (16) into Eqs. (14) and (15), yields

$$A_1\frac{d^4 W_n}{d\xi^4} + A_2\frac{\partial^2}{\partial \xi^2}\int_{-1/2}^{1/2} T^*\bar{z}\,d\bar{z} - \omega^2 W_n + 2cj\omega\frac{dW_n}{d\xi} + c^2\frac{d^2 W_n}{d\xi^2} = 0 \quad (\xi_{n-1} \le \xi \le \xi_n, \quad n = 1,2) \tag{17a}$$

$$\frac{d^2 T^*}{d\bar{z}^2} - A_3 j\omega T^* + A_4 j\omega\frac{d^2 W_n}{d\xi^2} = 0 \quad (\xi_{n-1} \le \xi \le \xi_n, \quad n = 1,2) \tag{17b}$$

where $A_1 = h^2/12L^2$, $A_2 = \alpha_T\tau_0$, $A_3 = h^2/aL\sqrt{E/\rho}$, $A_4 = E\alpha_T h^4/a\rho c_v L^3\sqrt{E/\rho}$,

$$W_1(\varsigma^-) = W_2(\varsigma^+)$$

$$\frac{dW_1(\varsigma^-)}{d\xi} = \frac{dW_2(\varsigma^+)}{d\xi}$$

$$\left[\frac{d^2 W_1(\varsigma^-)}{d\xi^2} - \frac{d^2 W_2(\varsigma^+)}{d\xi^2}\right] - \mu^2 F W_1'(\varsigma^-) - \mu K W_1(\varsigma^-) = 0 \tag{18}$$

$$\left[\frac{d^3 W_1(\varsigma^-)}{d\xi^3} - \frac{d^3 W_2(\varsigma^+)}{d\xi^3}\right] + 2KW_1(\varsigma^-) + 2\mu F W_1'(\varsigma^-) = 0$$

Both ends of the beam are assumed to be thermally insulated, so the boundary condition of the simply supported beam is

$$W|_{\xi=0} = W|_{\xi=1} = 0$$

$$\left.\frac{d^2 W}{d\xi^2}\right|_{\xi=0} = \left.\frac{d^2 W}{d\xi^2}\right|_{\xi=1} = 0 \tag{19}$$

$$T^*|_{\bar{z}=-1/2} = T^*|_{\bar{z}=1/2} = 0$$

The solution of Eq. (17*b*) can be obtained as

$$T^* = p_1 e^{r_1\bar{z}} + p_2 e^{-r_1\bar{z}} + \frac{E\alpha_T h^2}{\rho c_v L^2}\frac{d^2 W_n}{d\xi^2}\bar{z} \quad (\xi_{n-1} \le \xi \le \xi_n, \quad n = 1,2) \tag{20}$$

where p_1 and p_2 are two integral constants and $r_1 = \sqrt{A_3 j\omega}$.

Substituting Eq. (20) into Eq. (17*a*) leads to

$$(A_1 + \lambda)\frac{d^4 W_n}{d\xi^4} + c^2\frac{d^2 W_n}{d\xi^2} + 2cj\omega\frac{dW_n}{d\xi} - \omega^2 W_n = 0 \quad (\xi_{n-1} \le \xi \le \xi_n, \quad n = 1,2) \tag{21}$$

where $\lambda = E\alpha_T^2\tau_0 h^2/12a\rho c_v L^2$ is the dimensionless thermoelastic coupling factor. It represents the degree of the coupling between the temperature field and the strain field.

3 Differential Quadrature Method

The DQM [14] virtually is a method in which the derivatives of the function at the given nodes are approximately described by weighted sums of the function at the total nodes.

Consider a function of one variable $f(x)$; it is continuously differentiable in the interval $[a,b]$. There is a formula

$$L\{f(x)\} = \sum_{j=1}^{N} W_j(x) f(x_j) \tag{22}$$

where L is the linear differential operator, $W_j(x)$ is the interpolation basis functions, x_j is the coordinate value of the node j in the different nodes $a = x_1 < x_2 < \cdots < x_N = b$. If $L = d/dx$, $A_{ij} = W_j(x_i)$, and $f_j = f(x_j)$, then

$$f_i' = \sum_{j=1}^{N} A_{ij} f_j \quad (i = 1,2, \ldots, N) \tag{23}$$

A_{ij} is the weight coefficients of the first derivative of $f(x)$.

According the interpolation principle, the weight coefficients of the differential quadrature method are obtained by the differential coefficient of the Lagrange interpolation polynomial on the nodes. A_{ij} can be expressed as

$$A_{ij} = \begin{cases} \prod_{\substack{k=1 \\ k\neq i,j}}^{N} (x_i - x_k) \Big/ \prod_{\substack{k=1 \\ k\neq j}}^{N} (x_j - x_k) & (i,j = 1,2, \ldots, N; i \neq j) \\ \sum_{\substack{k=1 \\ k\neq i}}^{N} \dfrac{1}{(x_i - x_k)} & (i,j = 1,2, \ldots, N; i = j) \end{cases} \tag{24}$$

After A_{ij} is determined, B_{ij}, C_{ij}, and D_{ij} can be expressed as follows:

$$B_{ij} = \sum_{m=1}^{N} A_{im}A_{mj}, \quad C_{ij} = \sum_{m=1}^{N} B_{im}A_{mj}, \quad D_{ij} = \sum_{m=1}^{N} C_{im}A_{mj} \quad (i,j = 1,2,\ldots,N) \tag{25}$$

The simply supported beam adopts the weight coefficient method to treat the boundary conditions, and the contact point adopts the δ method to treat. The distribution forms of the nodes are

$$\xi_1 = 0, \quad \xi_N = 1, \quad \xi_i = \frac{1}{2}\left[1 - \cos\left(\frac{2i-3}{2N-4}\pi\right)\right] \quad (i = 2,3,\ldots,N-1)$$

$$\xi_p = \varsigma - 2\delta, \quad \xi_{p+1} = \varsigma - \delta, \quad \xi_{p+2} = \varsigma + \delta, \quad \xi_{p+3} = \varsigma + 2\delta \tag{26}$$

$$i \neq p, \quad i \neq p+1, \quad i \neq p+2, \quad i \neq p+3, \quad 1 \leq p \leq N-3$$

Based on the above statement, Eq. (21) can be rewritten in the differential quadrature form as

$$(A_1 + \lambda)\sum_{m=1}^{N} D_{im}W_{n,m} - \omega^2 W_{n,m} + 2c\mathrm{j}\omega\sum_{m=1}^{N} A_{im}W_{n,m} + c^2\sum_{m=1}^{N} B_{im}W_{n,m} = 0 \quad (n = 1,2) \tag{27}$$

The differential quadrature forms of the continuous condition (18) and boundary condition (19) are

$$W_{1p} - W_{2p} = 0$$

$$\sum_{m=1}^{N} A_{p+1,m}W_{1m} - \sum_{m=1}^{N} A_{p+1,m}W_{2m} = 0$$

$$\left[\sum_{m=1}^{N} B_{p+2,m}W_{1m} - \sum_{m=1}^{N} B_{p+2,m}W_{2m}\right] - \mu^2 F\sum_{m=1}^{N} A_{p+2,m}W_{1m} - \mu K W_{1m} = 0 \tag{28}$$

$$\left[\sum_{m=1}^{N} C_{p+3,m}W_{1m} - \sum_{m=1}^{N} C_{p+3,m}W_{2m}\right] + 2KW_{1m} + 2\mu F\sum_{m=1}^{N} A_{p+3,m}W_{1m} = 0$$

$$W_{11} = W_{2N} = 0$$

$$\sum_{m=1}^{N} B_{1m}W_{1m} = \sum_{m=1}^{N} B_{Nm}W_{2m} = 0 \tag{29}$$

Equation (27) and the boundary condition (29) can be written in the matrix form as

$$\begin{pmatrix} [Q_{dd}] & [Q_{de}] \\ [Q_{ed}] & [Q_{ee}] \end{pmatrix}\begin{pmatrix} \{y_d\} \\ \{y_e\} \end{pmatrix} + \omega\begin{pmatrix} 0 & 0 \\ [G_{ed}] & [G_{ee}] \end{pmatrix}\begin{pmatrix} \{y_d\} \\ \{y_e\} \end{pmatrix} + \omega^2\begin{pmatrix} 0 & 0 \\ 0 & [R] \end{pmatrix} \times \begin{pmatrix} \{y_d\} \\ \{y_e\} \end{pmatrix} = \begin{pmatrix} 0 \\ 0 \end{pmatrix} \tag{30}$$

where the subscript d denotes elements associated with the boundary points, while e is the remainder, namely,

$$\{y_d\} = \{y_1, y_2, y_{N-1}, y_N\}^T$$

$$\{y_e\} = \{y_3, y_4, \ldots, y_{N-3}, y_{N-2}\}^T \tag{31}$$

Equation (30) is rearranged into the following forms:

$$[Q_{dd}]\{y_d\} + [Q_{de}]\{y_e\} = 0 \tag{32}$$

Table 1 The first three order dimensionless natural frequencies

	ω_1	ω_2	ω_3	
Simply supported beam	0.2849	1.1396	2.5642	Present solution
	0.2849	1.1396	2.5639	Existing results [13]

$$[Q_{ed}]\{y_d\} + [Q_{ee}]\{y_e\} + \omega[G_{ed}]\{y_d\} + \omega[G_{ee}]\{y_e\} + \omega^2[R]\{y_e\} = 0 \tag{33}$$

Equation (32) can be rewritten in the form

$$\{y_d\} = -[Q_{dd}]^{-}[Q_{de}]\{y_e\} \tag{34}$$

Substituting Eq. (34) into Eq. (33), we then obtain

$$-[Q_{ed}][Q_{dd}]^{-}[Q_{de}]\{y_e\} + [Q_{ee}]\{y_e\} - \omega[G_{ed}][Q_{dd}]^{-}[Q_{de}]\{y_e\} + \omega[G_{ee}]\{y_e\} + \omega^2[R]\{y_e\} = 0 \tag{35}$$

We assume that

$$[Q] = [Q_{ee}] - [Q_{ed}][Q_{dd}]^{-}[Q_{de}]$$

$$[G] = [G_{ee}] - [G_{ed}][Q_{dd}]^{-}[Q_{de}] \tag{36}$$

then Eq. (35) can be written as

$$\{\omega^2[R] + \omega[G] + [Q]\}\{W_m\} = \{0\} \tag{37}$$

where the matrix $[Q]$, $[G]$, and $[R]$ involve several parameters, such as the dimensionless axially moving speed c, the dimensionless coupled thermoelastic factor λ, the dimensionless coefficient of spring stiffness K, and the friction coefficient μ. Equation (37) is a generalized eigenvalue problem. Then, the eigenequation for the axially moving beam of the coupled thermoelastic is

$$|\omega^2[R] + \omega[G] + [Q]| = 0 \tag{38}$$

4 Results and Discussions

Numerical studies have been conducted to investigate the effects of several key parameters on the dynamics and stabilities of the thermoelastic coupling axially moving beam. The first three order natural frequencies of the simply supported axially moving beam under $\mu=0$, $K=0$, $c=0$, $h/L=10$, and $\lambda=0$ are calculated. The results agree with those exhibited in Ref. [13], which can be seen in Table 1. Here, the node number $N=19$.

Figure 2 shows the variation in the first order dimensionless natural frequencies of the beam with the different thermoelastic coupling factor for $\varsigma=0.5$ and different other parameters. It can be seen that the first order dimensionless natural frequencies increase with the increase in the thermoelastic coupling factor under the different conditions $K=150$, $F=200$, $\mu=0$, and $\mu=0.3$.

Figure 3 shows the variation in the first order dimensionless complex frequencies of the beam with the dimensionless moving speed for $\varsigma=0.5$, $\lambda=0.1$, $\mu=0$, $F=200$, and the different values of the dimensionless spring stiffness K. It can be seen that when the dimensionless spring stiffness $K=0$, the critical divergence speed $c=3.31$; this is equal to the beam without the frictional contact. With the increase in the dimensionless spring stiffness K, the critical divergence speed increases; the first order mode behaves unstably due to the divergence instability. When the moving speed further increases to $c>6.63$, the real part of the ω in the first order mode becomes $\mathrm{Re}(\omega)>0$ and $\mathrm{Im}(\omega)<0$, which shows that the first order mode becomes unstable because of the flutter instability from the divergence instability.

Figure 4 shows the variation in the first order dimensionless complex frequencies of the beam with the dimensionless moving speed for $\varsigma=0.5$, $\lambda=0.1$, $F=200$, $K=10$, and the different values of the friction coefficient μ. It indicates that when the friction coefficient $\mu=0$, the real part of ω decreases with the increase in

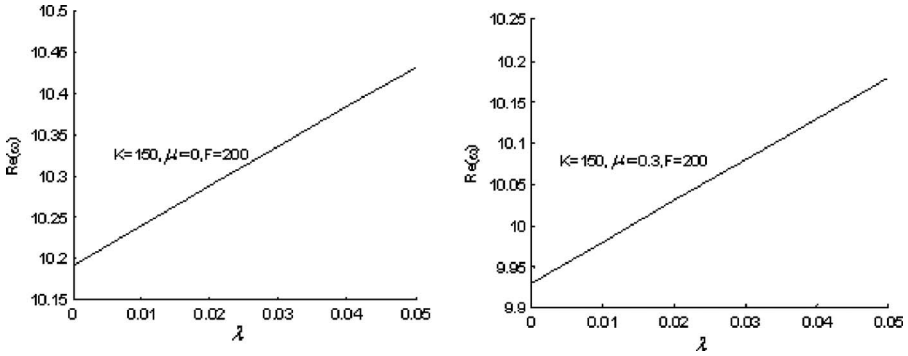

Fig. 2 The first order dimensionless natural frequencies versus the dimensionless thermoelastic coupling factor λ (ς=0.5)

the moving speed, while its imaginary part remains zero. When the moving speed increases to the critical value $c=3.45$, the real part of the ω in the first order mode becomes zero; subsequently, $\mathrm{Re}(\omega)=0$, but $\mathrm{Im}(\omega)>0$ and $\mathrm{Im}(\omega)<0$ occur, which shows that the first order mode becomes unstable because of the divergence instability. When the friction coefficient $\mu>0$, the real part of ω still decreases with the increase in moving speed, while its imaginary part is not zero but a negative value, namely, Re $\omega>0$, Im $\omega<0$. It indicates that the first order mode undergoes the flutter instability. With the increase in moving speed, the first order mode becomes unstable because of the flutter instability.

Figure 5 shows the variation in the first order dimensionless complex frequencies of the beam with the dimensionless moving speed for $\varsigma=0.5$, $\lambda=0.1$, $\mu=0.3$, $K=5$, and the different values of the dimensionless normal force F. It can be seen that when the dimensionless normal force $F>0$, the instability type of the system is equal to that in Fig. 4.

Figure 6 shows the variation in the first order dimensionless natural frequencies of the beam with the dimensionless spring stiffness for $\lambda=0.1$, $\mu=0$, $F=200$, and the different the frictional contact points ς. It can be seen that the first order dimensionless natural frequency increases with the increase in the dimensionless spring stiffness when the elastic supports are at the same point. These two lines coincide with each other at $\varsigma=0.4$ and $\varsigma=0.6$ ($\varsigma=0.1$ and $\varsigma=0.9$). The spring stiffness has the most influences on the first order dimensionless natural frequency when the frictional contact point is at the midpoint of the beam.

Figure 7 shows the variation in the first order dimensionless natural frequencies of the beam with the friction coefficient for $\lambda=0.1$, $K=10$, $F=200$, and the different frictional contact points ς. Figure 7 is different from Fig. 6, which contains the friction force. It can be seen that the variation tendencies of the first order dimensionless natural frequencies with the friction coefficient are different when the frictional contact points are at different points.

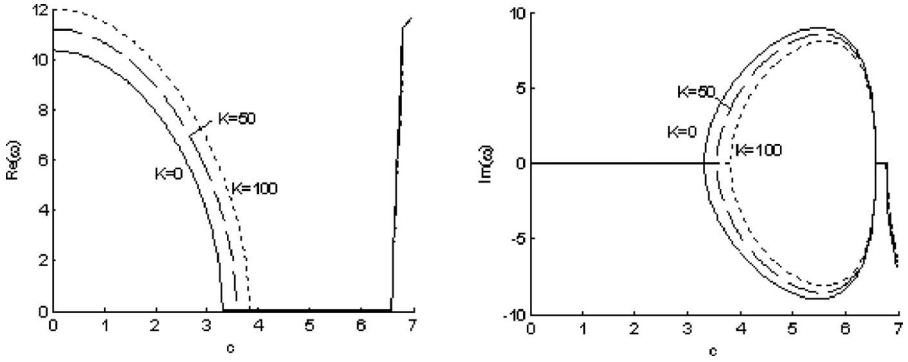

Fig. 3 The first order dimensionless complex frequencies versus the dimensionless axially moving speed for different *K* (ς=0.5, μ=0, *F*=200, and λ=0.1)

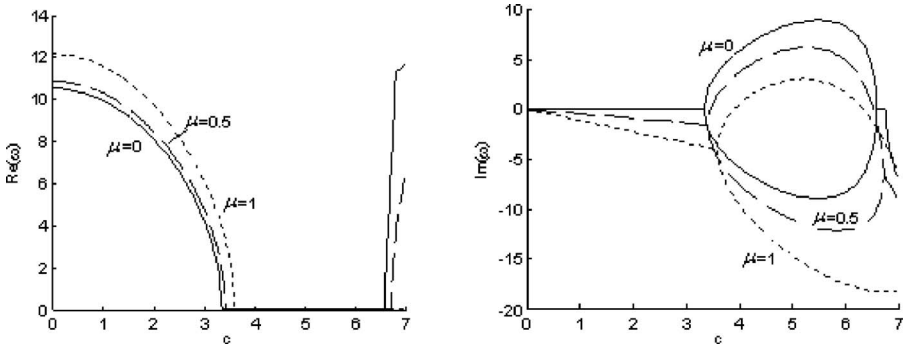

Fig. 4 The first order dimensionless complex frequencies versus the dimensionless axially moving speed for different μ (ς=0.5, *F*=200, *K*=10, and λ=0.1)

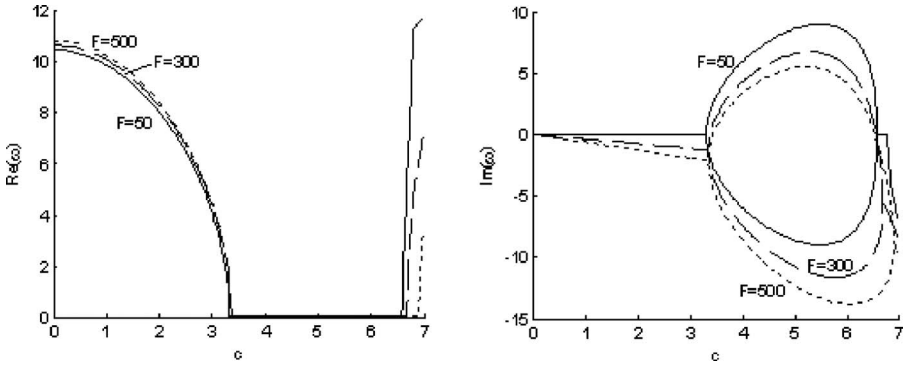

Fig. 5 The first order dimensionless complex frequencies versus the dimensionless axially moving speed for different F (ς=0.5, μ=0.3, K=5, and λ=0.1)

Figures 8 and 9 show the variation in the first order dimensionless natural frequencies of the beam with the different frictional contact points for μ=0 and μ=0.5. In Fig. 8, the first order dimensionless natural frequencies gradually increase when the frictional contact points move to the midpoint of the beam. The first order dimensionless natural frequencies get the maximum when the frictional contact point is at the midpoint; the first order dimensionless natural frequencies gradually decrease when the frictional contact points are removed from the midpoint of the beam. In Fig. 9, the first order dimensionless natural frequencies decrease first and increase later when the frictional contact points move to the midpoint of the beam. The first order dimensionless natural frequencies increase first and decrease later when the frictional contact points are removed from the midpoint of the beam. The first order dimensionless natural frequencies do not obtain the maximum when the frictional contact point is at the midpoint, but the minimum and the maximum appear at ς=0.3 and ς=0.7, respectively. The first order dimensionless natural frequencies increase with the increase in the spring stiffness in Figs. 8 and 9.

Figure 10 shows the variation in the first order dimensionless critical speed of the beam with the different spring stiffnesses under the cases for ς=0.5 and λ=0.1. It can be seen that the first order dimensionless critical speed increases with the increase in the spring stiffness under the two cases. When $K<61.9$, the first order dimensionless critical speed under μ=0.5 and F=200 is greater than that under μ=0 and F=200; the conclusion was the contrary when $K>61.9$.

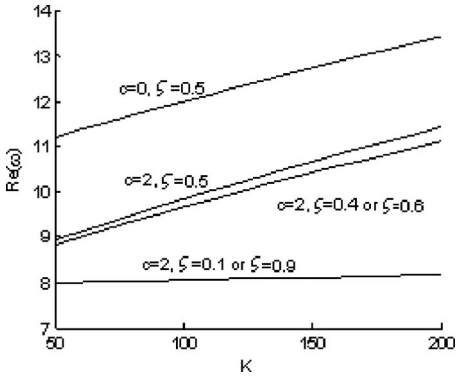

Fig. 6 The first order dimensionless natural frequencies versus K for different ς (μ=0, F=200, and λ=0.1)

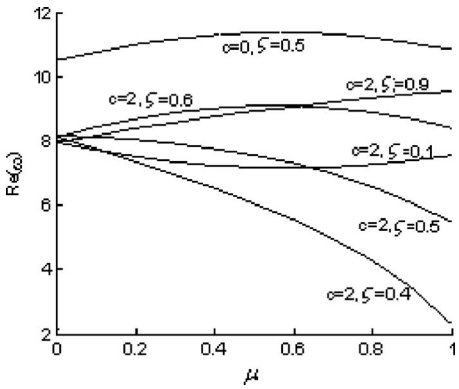

Fig. 7 The first order dimensionless natural frequencies versus μ for different ς (F=200, K=10, and λ=0.1)

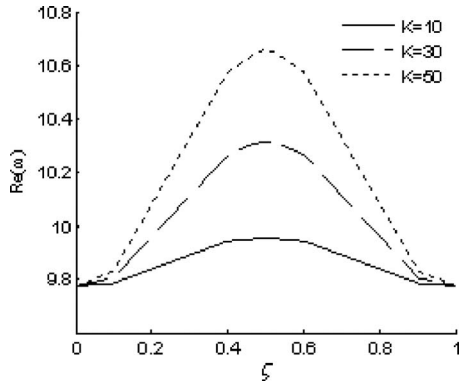

Fig. 8 The first order dimensionless natural frequencies versus ς (μ=0, F=200, c=1, and λ=0.1)

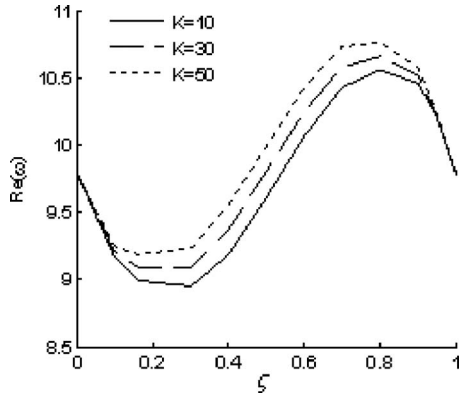

Fig. 9 The first order dimensionless natural frequencies versus ς (μ=0.5, F=200, c=1, and λ=0.1)

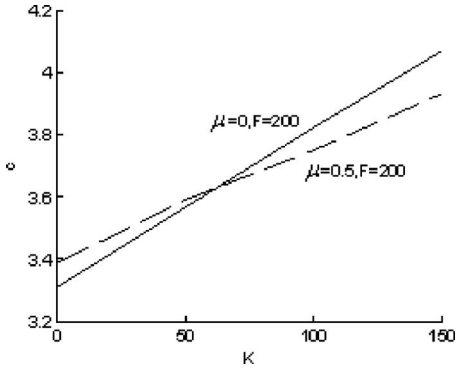

Fig. 10 The first order dimensionless critical speed versus K ($\varsigma=0.5$ and $\lambda=0.1$)

Figure 11 shows the variation in the first order dimensionless critical speed of the beam with the friction coefficient for $\varsigma=0.5$, $\lambda=0.1$, $K=10$, and $F=200$. It indicates that the first order dimensionless critical speed increases with the increase in the friction coefficient.

5 Conclusions

This paper calculates the dimensionless complex frequencies of the axially moving beam under the thermoelastic coupling case with the frictional contact by the differential quadrature method. The effects of the each parameter on the stability of the beam are analyzed. The results of the analysis of the present study can be summarized as follows:

1. The real parts of the first three complex frequencies in the thermoelastic coupling case $\lambda \neq 0$ are greater than that in the case of uncoupling when the other conditions are constants. The first order dimensionless natural frequencies increase with the increase in the thermoelastic coupling factor.
2. The first order dimensionless natural frequencies increase with the increase in the dimensionless spring stiffness when the elastic supports are at a fixed point in the cases $\mu=0$ and $\mu \neq 0$, but the instability type of the system is different. The first order dimensionless natural frequencies reach the maximum when the frictional contact point is at the midpoint when the friction coefficient is zero. Otherwise, the first order dimensionless natural frequencies obtain the minimum and the maximum at $\varsigma=0.3$ and $\varsigma=0.7$, respectively.
3. In the case $\mu \neq 0$, the critical flutter speed of the first order mode increases with the increase in the friction coefficient or the normal force, and the system behaves according to the single mode flutter instability.

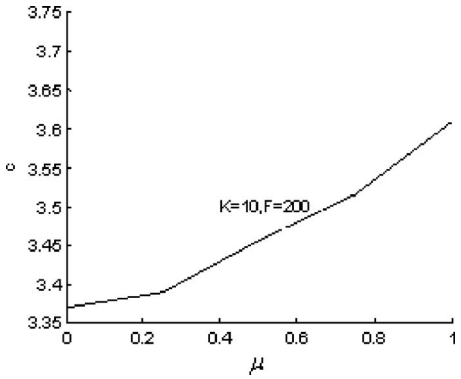

Fig. 11 The first order dimensionless critical speed versus μ ($\varsigma=0.5$ and $\lambda=0.1$)

Acknowledgment

The authors gratefully acknowledge the support of the National Natural Science Foundation of China (Grant No. 10872163) and the Natural Science Foundation of Education Department of Shaanxi Province of China (Grant No. 08JK394).

References

[1] Simpson, A., 1973, "Transverse Modes and Frequencies of Beams Translating Between Fixed and Supported," J. Mech. Eng. Sci., **15**(3), pp. 159–164.
[2] Wickert, J. A., and Mote, C. D., 1990, "Classical Vibration Analysis of Axially Moving Continua," ASME J. Appl. Mech., **57**, pp. 738–744.
[3] Wickert, J. A., and Mote, C. D., 1991, "Response and Discretization Methods for Axially Moving Materials," ASME J. Appl. Mech., **44**, pp. S279–S284.
[4] Chakraborty, G., and Mallik, A. K., 2000, "Wave Propagation in and Vibration of a Traveling Beam With and Without Non-Linear Effects," J. Sound Vib., **236**(2), pp. 277–290.
[5] Kong, L., and Parker, G., 2004, "Approximate Eigensolutions of Axially Moving Beams With Small Flexural Stiffness," J. Sound Vib., **276**(1–2), pp. 459–469.
[6] Yang, X. D., and Chen, L. Q.2007, "Determination of the Natural Frequencies of Axially Moving Beams by the Method of Multiple Scales," J. Shanghai Univ., **11**(3), pp. 251–254.
[7] Avsec, J., and Oblak, M., 2007, "Thermal Vibrational Analysis for Simply Supported Beam and Clamped Beam," J. Sound Vib., **308**(3–5), pp. 514–525.
[8] Manoach, E., and Ribeiro, P., 2004, "Coupled, Thermoelastic, Large Amplitude Vibrations of Timoshenko Beams," Int. J. Mech. Sci., **46**(11), pp. 1589–1606.
[9] Chang, W. P., and Wan, S. M., 1986, "Thermomechanically Coupled Nonlinear Vibration of Plates," Int. J. Non-Linear Mech., **21**(5), pp. 375–389.
[10] Eslami, M. R., Shakeri, M., and Sedaghati, R., 1994, "Coupled Thermoelasticity of Axially Symmetric Cylindrical Shell," J. Therm. Stresses, **17**(1), pp. 115–135.
[11] Copper, C. D., and Pilkey, W. D., 2002, "Thermoelasticity Solutions for Straight Beams," ASME J. Appl. Mech., **69**(5), pp. 224–229.
[12] Guo, F. L., and Rogerson, G. A., 2003, "Thermoelastic Coupling Effect on a Micro-Machined Beam Resonator," Mech. Res. Commun., **30**(6), pp. 513–518.
[13] Sun, Y. X., Fang, D. N., and Ai, K. S., 2006, "Thermoelastic Damping in Micro-Beam Resonators," Int. J. Solids Struct., **43**(10), pp. 3213–3229.
[14] Guo, X. X., Wang, Z. M., Wang, Y., and Zhou, Y. F., 2009, "Analysis of the Coupled Thermoelastic Vibration for Axially Moving Beam," J. Sound Vib., **325**(3), pp. 597–608.
[15] Kang, B., and Tan, C. A., 2004, "Parametric Instability of a Leipholz Beam Due to Distributed Frictional Axial Load," Int. J. Mech. Sci., **46**(6), pp. 807–825.
[16] Cheng, S. P., and Perkins, N. C., 1991, "The Vibration and Stability of a Friction-Guided, Translating String," J. Sound Vib., **144**(2), pp. 281–292.
[17] Chen, J. S., 1997, "Natural Frequencies and Stability of an Axially-Traveling String in Contact With a Stationary Load System," ASME J. Vibr. Acoust., **119**, pp. 152–157.
[18] Adams, G. G., 1996, "Self-Excited Oscillations in Sliding With a Constant Friction Coefficient—A Simple Model," ASME J. Tribol., **118**, pp. 819–823.
[19] Mottershead, J. E., and Chan, S. N., 1995, "Flutter Instability of Circular Discs With Frictional Follower Loads," ASME J. Vibr. Acoust., **117**, pp. 161–163.
[20] Daniel, H., Gottfried, S. K., and Peter, H., 2007, "Friction Induced Vibrations in Moving Continua and Their Application to Brake Squeal," ASME J. Appl. Mech., **74**, pp. 542–549.
[21] Gottfried, S. K., Kirillov, O. N., and Peter, H., 2008, "Modeling and Stability Analysis of an Axially Moving Beam With Frictional Contact," ASME J. Appl. Mech., **75**, p. 031001.